

Non-SM Exotic Higgs: Beyond SM and MSSM

Stefano Lacapra^{1, a} on behalf of ATLAS, CDF, CMS and D0 collaboration

¹INFN Sez. Padova, via Marzolo, 8, 35131 Padova Italy

Abstract. A review of the searches for exotic Higgs boson beyond standard model and minimal supersymmetric standard model (MSSM), from experiments at the Tevatron and LHC, is presented. Several different models have been considered, including extensions to standard model with fourth generation of fermions, fermiophobic Higgs, next-to-MSSM models, seesaw type-II, and rare decay of Higgs boson to hidden sector. For next-to-MSSM models several final states have been considered, including light pseudo-scalar Higgs decay into taus, muons, and photons, as well as charged Higgs boson. The searches has been performed with re-interpretation of results from standard model Higgs search as well as on new signatures.

1 Introduction

The recent discovery of a new particle in the search for Standard Model (SM) Higgs boson by CMS [1] and ATLAS [2] collaboration at the LHC is possibly the last missing stone of the SM building. The precise nature of this new particle is however still being investigated. Moreover, the SM is well known to break at a larger scale and some major open points must be understood: the unification of couplings; hierarchy problem; the dark matter issue; and the source of neutrino masses. In relation to these aspects, searches for an extended Higgs sector, with additional Higgs-like particles, is of great interest.

This report summarizes some of the searches performed at hadron colliders for an Higgs-like particle beyond the SM, and beyond the Minimal Supersymmetric Standard Model (MSSM). Different scenarios are considered: a standard model with a fourth generations of fermions (SM4); a fermiophobic Higgs scenario; several searches in the context of the next-to MSSM (NMSSM) framework, including charged Higgs, light pseudo-scalar Higgs decaying into a pair of muons, or pairs of photons; doubly charged Higgs bosons predicted by the minimal type II seesaw model; and searches of rare Higgs decay into hidden sector. Results both from Tevatron (CDF [3] and D0 [4] collaborations) and LHC (ATLAS [5] and CMS [6]) are presented.

2 Higgs in Standard Model with 4th generation

In the SM there are three generations of fermions, but the model can be extended by a fourth generation (SM4) [7]. The existence of these new fermions (u_4, d_4, ℓ_4, ν_4) is not excluded by direct searches and precision EWK measurements, provided that the fermions are

heavy enough and the mass split between u_4 and d_4 is not too large ($O(50)$ GeV). The presence of a fourth generation has profound implication for the phenomenology of the Higgs sector at hadron colliders: in particular, the production cross section via the gluon fusion process is enhanced by almost an order of magnitude, due to the presence of fourth generation quarks in the loop mediating the gluon fusion $gg \rightarrow H$ diagram. Other production processes become negligible by comparison. The Higgs boson production is not associated to other tags, such as forward jets, as in vector boson fusion (VBF) production mechanism, or additional vector boson, as in Higgs-strahlung (VH) processes. The branching fraction into photons is largely suppressed, due to a cancellation of SM and SM4 diagrams, while that into vector bosons is smaller, and into fermions is larger by approximately 60%. The changes in the production cross section and decay fraction require a reinterpretation of the SM search in the context of SM4.

At the Fermilab Tevatron, CDF and D0 [8], using an integrated luminosity $L = 8.2 \text{ fb}^{-1}$, have investigated two SM4 scenarios: *low mass*, where $m_{\nu_4} = 80 \text{ GeV}$, $m_{\ell_4} = 100 \text{ GeV}$ and *high mass* where $m_{\nu_4} = m_{\ell_4} = 1 \text{ TeV}$. In both cases $m_{d_4} = 400 \text{ GeV}$ and $m_{u_4} = m_{d_4} + (50 + 10 \cdot \ln(m_H/115)) \text{ GeV}$. The search uses only Higgs decay into two W bosons, considering a final state with leptonic decay for both the W, with a charged, isolated, high momentum lepton and large transverse imbalanced momentum (MET). The two scenarios predict a cross section times branching fraction larger than the SM one for $gg \rightarrow H \rightarrow WW$, with small difference for $m_H \gtrsim 160 \text{ GeV}$. No excess over the expected background has been reported, and the Higgs boson mass range $124 < m_{H_{SM4}} < 286$ has been excluded at 95% confidence level (CL).

At LHC, ATLAS [9], using $L = 1.0\text{-}2.3 \text{ fb}^{-1}$, and CMS [10], using $4.6\text{-}4.8 \text{ fb}^{-1}$, both at $\sqrt{s} = 7 \text{ TeV}$, have explored a slightly different scenario, with $m_{\ell_4} = m_{\nu_4} = m_{d_4} = 600 \text{ GeV}$, and the same $m_{u_4} - m_{d_4}$ as that used at

a. e-mail: stefano.lacapra@pd.infn.it

Tevatron. The analysis uses all the final states accessible at LHC for the SM Higgs search: $H \rightarrow \tau\tau$, which is dominant at low m_H ; $H \rightarrow WW$; and $H \rightarrow ZZ$. The other possible channels, $H \rightarrow \gamma\gamma, bb$, have very little sensitivity for a SM4 Higgs boson. ATLAS excludes $120 < m_{H_{SM4}} < 600$ GeV at 95% CL. Figure 1 shows the CMS upper limit on signal strength μ , defined as the ratio of the observed (or expected) cross section relative to that expected for SM4 Higgs boson ($\mu = \sigma/\sigma_{SM4}$). The whole mass range (110-600 GeV) was expected to be excluded in the case that there is no SM4 Higgs boson, while the observed exclusion is in the range $123 < m_{H_{SM4}} < 600$ GeV.

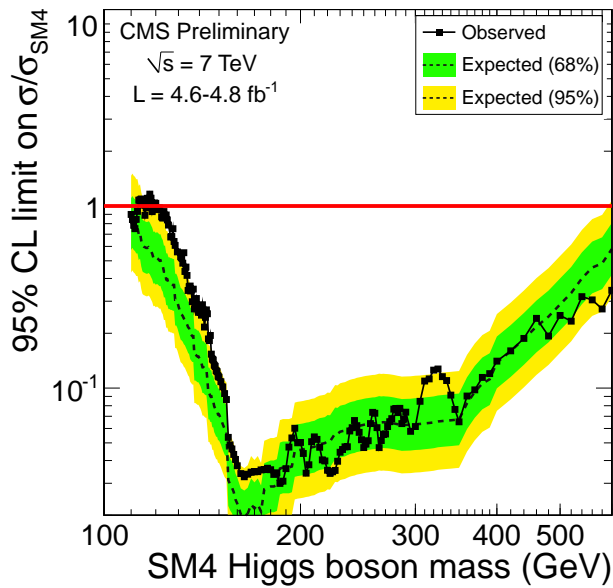


Figure 1. Exclusion plot at 95% for signal strength σ/σ_{SM4} for Standard Model with a fourth generation of fermions as a function Higgs boson mass, as obtained by CMS [10].

3 Fermiophobic Higgs

A fermiophobic Higgs boson is a SM-like boson which is coupled only to bosons, and not to fermions. This behaviour is possible in the SM with an extended Higgs sector, for example in models with two Higgs doublet (2HDM). In this model the decays of the Higgs boson are obviously changed with respect to the SM case, since it only decays into $\gamma\gamma$, WW , and ZZ are allowed. Also the production is deeply affected, though, since the major production mechanism (gluon fusion) which is mediated by a fermion (t) loop, is forbidden. Also the smaller $t\bar{t}$ associated production is not possible. The dominant production channels become vector boson fusion and Higgsstrahlung. The Higgs boson produced by these two processes is boosted, and is associated to additional signature in the final state, such as forward-backward jets, leptons, and MET (from V decay). Direct searches performed at LEP give an upper bound on H mass $m_H < 108.2$ GeV [11].

A search for fermiophobic Higgs boson has been done at CDF and D0 [12], using $L = 8.2$ fb^{-1} for each experiment. The analyses re-use the SM searches with an optimization to make use of these additional signatures. The final states considered include $H \rightarrow \gamma\gamma$ as well as $H \rightarrow WW$ with jets or an additional W/Z . The combined analysis for the two experiments sees no excess and sets a lower limit for $m_H < 119$ GeV 95% CL.

At LHC, the ATLAS collaboration [13] considered the $H \rightarrow \gamma\gamma$ final states, using $L=4.9$ fb^{-1} . The data is divided into a number of sub-channels, exploiting the Higgs boson boost. In particular, Higgs boson decay is searched for in events with low and high $P_T^{\gamma\gamma}$, which is defined as the transverse momentum of the $\gamma\gamma$ system orthogonal to the $\gamma\gamma$ thrust axis. This variable is sensitive to the boost of the Higgs boson, but less sensible to mismeasurement of the energy of one of the two γ with respect to the transverse momentum of the system of the two photons. An excess corresponding to 1.6σ significance is observed for $m_H = 125.5$ GeV, once the look-elsewhere effect is taken into account, and is interpreted in the context of SM Higgs search. No other significant deviations from expected background are seen, and the regions $m_H \in [110 - 118] \cup [119.5 - 121]$ GeV are excluded at 95% CL.

In CMS, a similar analysis has been performed [10, 14], with a statistics corresponding to $4.9\text{-}5.1$ fb^{-1} at $\sqrt{s} = 7$ TeV, considering $H \rightarrow WW$ and $H \rightarrow ZZ$ final states, and with $5.1(5.3)$ fb^{-1} , at $\sqrt{s} = 7(8)$ TeV considering the $H \rightarrow \gamma\gamma$ decay. The latter decay mode is used in association with a pair of backward-forward jets (expected in VBF production), isolated muon/electron or large MET (as in VH processes), or large Higgs boson boost (in both VBF and VH). To exploit the boost feature, a two dimensional analysis is performed, using the invariant mass of the two photons and $p_T^{\gamma\gamma}/m_{\gamma\gamma}$. The largest excess, found at $m_H = 125.5$ GeV has a probability corresponding to 3.2σ of a left-sided Gaussian distribution to be a background fluctuation (without the look-elsewhere-effect) but has a signal strength too low to be compatible with a fermiophobic hypothesis. An upper limit of $m_H < 147$ GeV at 95% CL has been set, as shown in Fig. 3.

4 Next to Minimal Supersymmetric Standard Model

Supersymmetry is one of the favourite extensions of the SM, thanks to its ability to solve some of the SM problems. The next-to MSSM model [15] (NMSSM) adds a further scalar singlet to the Higgs sector of the MSSM. It has some advantage over the MSSM, since it accommodates better for an Higgs boson with a mass $m_H = 125 - 126$ GeV. Furthermore, it solves the problem of the μ -term in the lagrangian of the theory, since that term is dynamically produced by a vacuum expectation value of the singlet, avoiding the need of fine-tuning. The resulting Higgs sector in the NMSSM comprises three CP-even states $h_{1,2,3}$, two CP-odd ones $a_{1,2}$, and two charged H^\pm . The a_1 is a superposition of the MSSM doublet pseu-

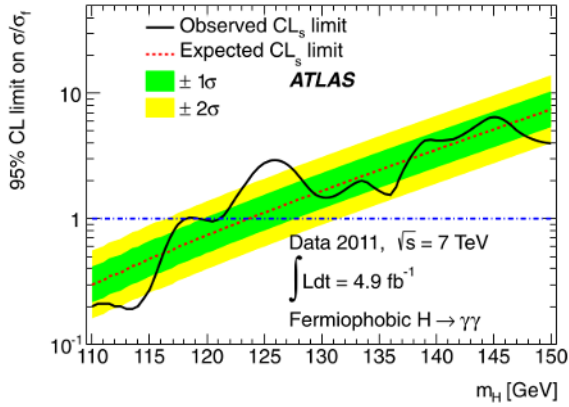


Figure 2. Observed and expected limit at 95% CL for a fermiophobic higgs production and decay $\sigma/\sigma_{\text{FP}}$ as a function Higgs boson mass, as obtained by ATLAS [13].

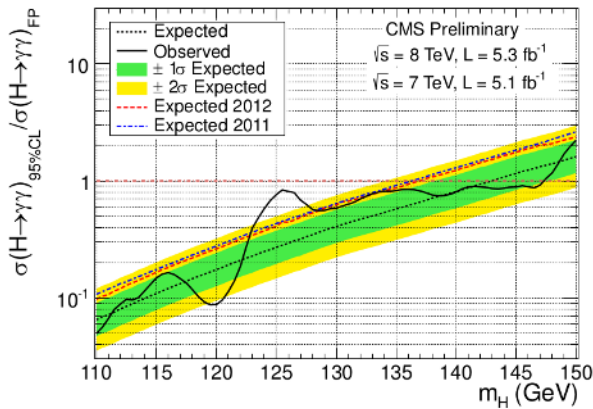


Figure 3. Exclusion plot at 95% for a fermiophobic higgs production and decay $\sigma/\sigma_{\text{FP}}$ as a function Higgs boson mass, as obtained by CMS [10, 14].

doscalar (a_{MSSM}) and the additional singlet pseudoscalar of the NMSSM (a_S): $a_1 = \cos \theta_A \cdot a_{\text{MSSM}} + \sin \theta_A \cdot a_S$, where θ_A is the mixing angle between the two pseudoscalars. In the context of the NMSSM, the a_1 can be very light $m_{a_1} \lesssim 2m_b$ and be nearly pure a_S ($\cos \theta_A \ll 1$), and can have a significant branching ratio to photons, muons, taus, and bottom quarks for large $\tan \beta$ [16], where $\tan \beta$ is the ratio of the vacuum expectation values for the two MSSM Higgs doublets, depending on the kinematically allowed decay channel for a given a_1 mass. Several of these final states have been searched for at hadron colliders.

4.1 $t \rightarrow H^\pm b \rightarrow (W^\pm a_1) b, a_1 \rightarrow \tau \tau$

If the charged Higgs boson has a mass below that of the top quark, one possible decay chain is the following: $t \rightarrow H^\pm b \rightarrow (W^\pm a_1) b$. At CDF this channel has been explored, looking for a_1 decay into a pair of τ , using $L=2.7 \text{ fb}^{-1}$ [17]. The final state resembles the $t\bar{t}$ process, with only the addition of isolated τ 's. The event selection follows the standard $t\bar{t}$ one, requiring an isolated electron

or muon plus missing energy from the decay of one of the W 's, and three jets, one of which is b -tagged. The τ signature is searched for in the 1-prong decay, by looking at one isolated track away from the lepton. The final selection makes use of the isolated track transverse momentum distribution to distinguish the a_1 signal from the dominant background coming from underlying events. No excess is observed, and a lower limit on the $\mathcal{B}(t \rightarrow H^\pm a_1)$ is set, as shown in Fig. 4, for a charged Higgs boson mass in range $90 < m_H^\pm < 160 \text{ GeV}$ and for four different values of $m_{a_1} = 4 - 9 \text{ GeV}$, assuming 100% branching fraction for $H^\pm \rightarrow W^\pm a_1$ and $a_1 \rightarrow \tau \tau$.

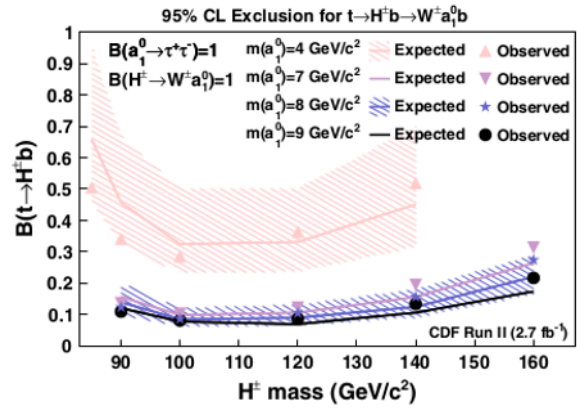


Figure 4. CDF exclusion plot at 95% for $t \rightarrow H^\pm b \rightarrow (W^\pm a_1) b$, and $a_1 \rightarrow \tau \tau$ as a function H^\pm mass and for four different values of m_{a_1} [17].

4.2 $h \rightarrow aa \rightarrow 4\mu$

Another possible production chain is $pp \rightarrow h \rightarrow aa \rightarrow 4\mu$, which has been investigated by CMS [18] with $L=5.3 \text{ fb}^{-1}$. The h production is via the gluon fusion process. The final state signature is quite simple, with two pairs of oppositely charged muons with the same invariant mass, since each pair comes from the decay of the same state a_1 . The selection requires four muons with relatively large transverse momentum, $p_T > 17 \text{ GeV}$ and $|\eta| < 0.9$ for the leading and $p_T > 8 \text{ GeV}$ and $|\eta| < 2.4$ for the other three, all isolated and coming from the same vertex. A possible signal is searched for when the invariant masses of the two pairs are close $m_1 \approx m_2$, and the sidebands ($m_1 \neq m_2$) provide a control sample to estimate the background from resonances ($\omega, \rho, \phi, J/\psi, \dots$). No excess over background has been observed, and a limit on $\sigma(pp \rightarrow h \rightarrow a_1 a_1) \times \mathcal{B}^2(a_1 \rightarrow 2\mu) \lesssim 5 - 2 \text{ fb}$ is set, depending on $m_H = 80 - 150 \text{ GeV}$, as shown in Fig. 6 (right). A similar analysis has been published by D0, with $L=4.2 \text{ fb}^{-1}$ [19], considering for the final state also the possibility that one of the a_1 decays into a pairs of τ . The results are summarized in Fig. 5.

CMS results can also be interpreted in the context of dark-SUSY models [20], where the decay chain of the initial h state is the following: $h \rightarrow 2n_1$, where n_1 is the

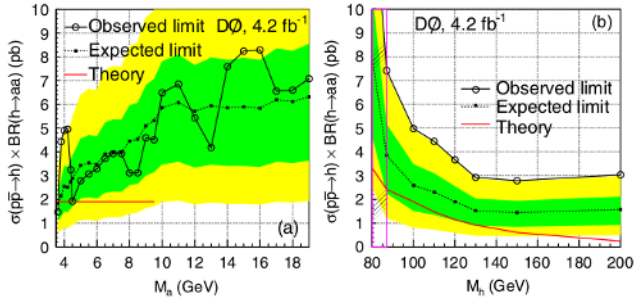


Figure 5. D0 exclusion plot at 95% for $\sigma(\text{pp} \rightarrow h \rightarrow a_1 a_1) \times \mathcal{B}^2(a_1 \rightarrow 2\mu)$ as a function of m_{a_1} (left) and m_h (right) [19].

SUSY lightest neutralino, which is not stable but decays $n_1 \rightarrow \gamma_D + n_D$ into a dark-photon and a dark-neutralino. The latter dark-particle is stable and escapes detection, while the γ_D decays into a pair of μ , leading to a final state very similar to that of NMSSM. The results are shown in Fig. 6 (left). A similar analysis done by ATLAS is described in Sec. 5.2.

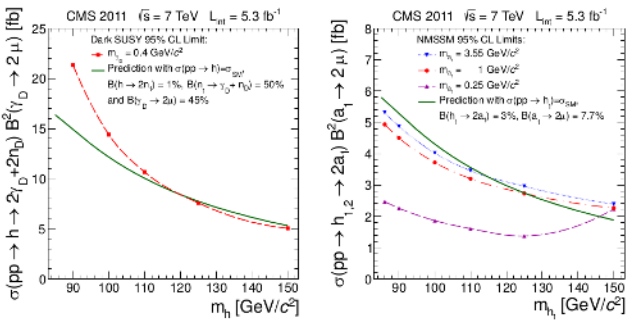


Figure 6. CMS exclusion plot at 95% for $\sigma(\text{pp} \rightarrow h \rightarrow 2n_D 2\gamma_D) \times \mathcal{B}(\gamma_D \rightarrow \mu\mu)$ (left) and $\sigma(\text{pp} \rightarrow h \rightarrow a_1 a_1) \times \mathcal{B}^2(a_1 \rightarrow 2\mu)$ (right) as a function m_h and for four different values of m_{a_0} [18].

4.3 $gg \rightarrow a \rightarrow 2\mu$

A direct search for $gg \rightarrow a \rightarrow \mu\mu$ has been performed near the Υ family of resonances at CDF [21] with $L = 0.63 \text{ fb}^{-1}$ and CMS [22] with $L = 1.3 \text{ fb}^{-1}$. In both cases a highly dedicated trigger was used to collect data, requiring two oppositely charged muons, with very low transverse momentum and coming from the same vertex, and with an invariant mass $m_{\mu\mu}$ close to that of the Υ : for CDF $m_{\mu\mu} \in [6.3 - 9] \text{ GeV}$, while CMS investigated also the region above the Υ $m_{\mu\mu} \in [5.5 - 8.8] \cup [11.5 - 14] \text{ GeV}$. A continuous background is expected from QCD as well as from the residual tail of the Υ decay. No peak over the background is seen in either analyses. CDF set an upper limit on $\sigma \times \mathcal{B}(a_1 \rightarrow \mu\mu)/\sigma \times \mathcal{B}(\Upsilon(1s) \rightarrow \mu\mu)$, as shown in Fig. 7, while CMS set an upper limit, shown in Fig. 8, directly on the cross section $\sigma(gg \rightarrow a)\mathcal{B}(a \rightarrow \mu\mu)$.

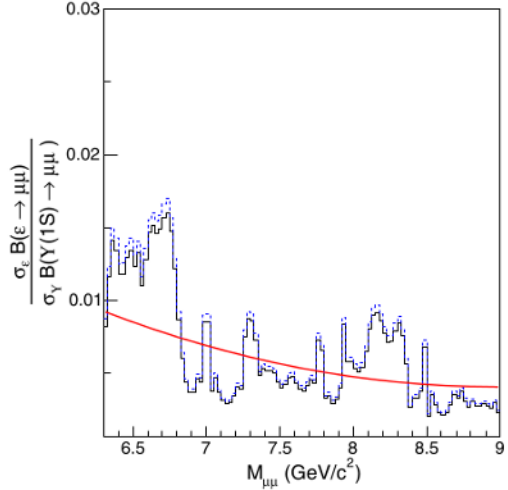


Figure 7. CDF exclusion plot at 90% (solid histogram) for $\sigma \times \mathcal{B}(a_1 \rightarrow \mu\mu)/\sigma \times \mathcal{B}(\Upsilon(1s) \rightarrow \mu\mu)$ for the mass range $m_{\mu\mu} \in [6.3 - 9] \text{ GeV}$. The dashed histogram represents limits that include the 6% systematic uncertainty. The red line represents the expected limits in case of no signal [21].

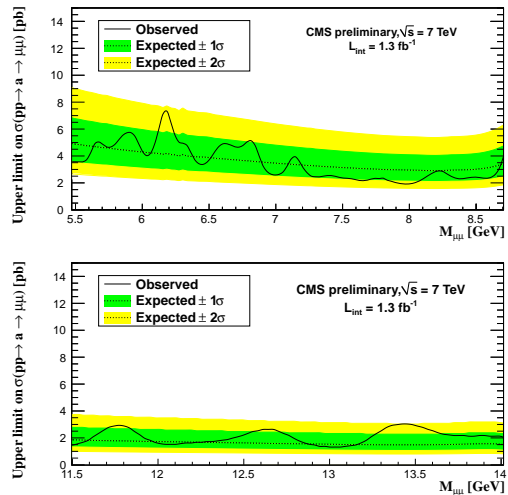


Figure 8. CMS exclusion plot at 95% for $\sigma_a \mathcal{B}(a \rightarrow \mu\mu)$ for the two mass range 5.5-8.8 GeV and 11.5-14 GeV [22].

4.4 $h \rightarrow aa \rightarrow 4\gamma$

A very light a_1 , with $m_a < 3m_{\pi^0}$, would have the decay into a pair of photons enhanced, resulting in a very clean signal. The ATLAS collaboration has searched [23] for such a signal in the decay chain $pp \rightarrow h \rightarrow aa \rightarrow (\gamma\gamma) + (\gamma\gamma)$, using $L = 4.9 \text{ fb}^{-1}$. The large boost of the a_1 makes the resulting two γ 's from one a_1 decay to be very collinear and hardly distinguishable within the detector resolution. As a consequence, the experimental signature is quite similar to that of the SM $H \rightarrow \gamma\gamma$, so that analysis can be reused, by just relaxing the shower shape requirements on the γ , allowing for a larger lateral energy leak than the single γ in the SM analysis. No significant deviation from the continuous background has been observed, and an upper limit on

cross section $\sigma(h \rightarrow aa \rightarrow 4\gamma) \lesssim 0.1 - 0.3$ pb for h masses in the range 110-150 GeV and for three different values of $m_a = 100, 200, 400$ MeV. As an example, the upper limit for $m_a = 200$ MeV is shown in Fig. 9

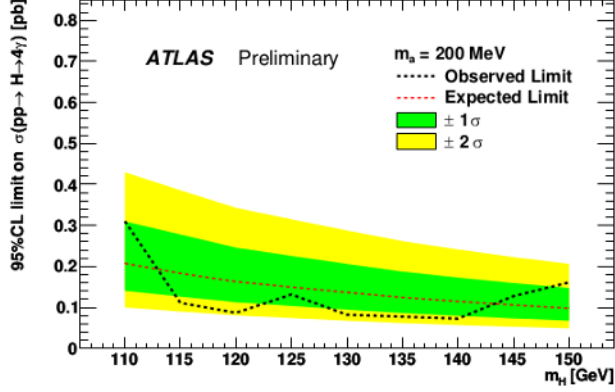


Figure 9. ATLAS exclusion plot at 95% for $\sigma(h \rightarrow aa \rightarrow 4\gamma)$ vs m_h [23].

5 Exotic

5.1 See-Saw Type-II H^{++}

The minimal seesaw model of type II [24] includes in the SM Higgs sector an additional scalar field, which acts as a triplet under $SU(2)_L$. This triplet produces a set of Higgs boson-like particles: neutral; charged; and doubly charged $\Phi^0, \Phi^+, \Phi^{++}$. The Yukawa coupling matrix element of these scalar field are proportional to the light neutrino mass matrix. They decay into leptons, including flavour-violating decay. The decay of Φ^{++} is into pair of same-charge leptons, for which the SM background is highly suppressed. The production is via vector boson: $W \rightarrow \Phi^{++}\Phi^-$ and $Z\gamma \rightarrow \Phi^{++}\Phi^{--}$ with a final state with many leptons, with an unique resonant same-sign leptons signature. The observation of $\Phi^{\pm\pm} \rightarrow \ell_i^\pm \ell_j^\pm$ decays at the LHC would allow testing of the neutrino mass mechanism, including the absolute mass scale, hierarchy, and CP-violating phases.

The ATLAS collaboration analyzed $L=4.7 \text{ fb}^{-1}$ of data at $\sqrt{s} = 7 \text{ TeV}$ [25], looking for final states with electrons or muons, without finding any significant peak structure over the SM background. A lower limit on the mass of the $m_{\Phi^{\pm\pm}} < 409 - 367 \text{ GeV}$ at 95% CL for final states $e^\pm e^\pm / \mu^\pm \mu^\pm / e^\pm \mu^\pm$, assuming 100% branching fraction of the $\Phi^{\pm\pm} \rightarrow \ell^\pm \ell^\pm$. An example for the $\mu^\pm \mu^\pm$ final state is shown in Fig. 10.

CMS has performed a similar analysis with $L=4.6 \text{ fb}^{-1}$ [26], considering in the final states also τ^\pm with hadronic decay, in addition to electrons and muons. No signal has been found in any final state, and lower limits have been set $m_{\Phi^{\pm\pm}} < 455$ for e^\pm and μ^\pm combinations; $m_{\Phi^{\pm\pm}} < 350$ for e^\pm / μ^\pm plus τ_h^\pm ; and $m_{\Phi^{\pm\pm}} < 200$ for τ_h^\pm only final state. In all cases, a 100% branching fraction of the $\Phi^{\pm\pm} \rightarrow \ell^\pm \ell^\pm$ is assumed. Four benchmark

scenarios have been also considered: normal hierarchy for neutrino masses; inverted hierarchy; a scenario where all neutrino masses are degenerate; and one where all the branching fractions to leptons are equal. The limits are summarized in Fig. 11.

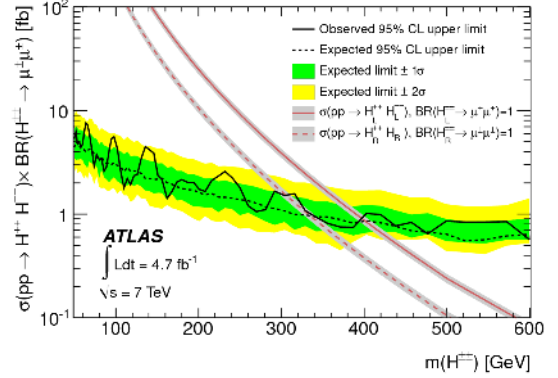


Figure 10. ATLAS upper limit on $\sigma(pp \rightarrow \Phi^{++}\Phi^{--}) \times \mathcal{B}(\Phi^{\pm\pm} \rightarrow \mu^\pm \mu^\pm)$ as a function of $m_{\Phi^{\pm\pm}}$ at 95% CL. The two lines represent the expected $\sigma \times \mathcal{B}$ for two different types of H^{++} : left-handed and right-handed. The crossing of those lines with the observed limit set a lower limit for the $\Phi^{\pm\pm}$ mass for that specific model [25].

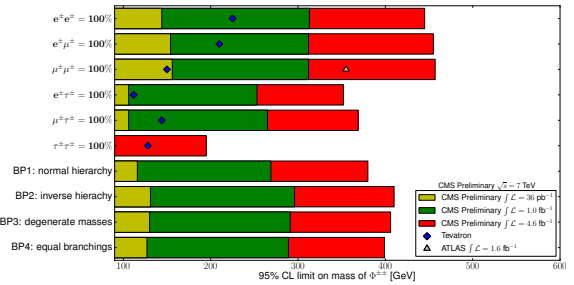


Figure 11. CMS lower limits on $m_{\Phi^{\pm\pm}}$ at 95% for different final states, and different benchmark scenarios, assuming $\mathcal{B}(\Phi^{\pm\pm} \rightarrow \ell^\pm \ell^\pm) = 100\%$ [26]. Previous results from D0 [27] and CDF [28] are also represented.

5.2 Hidden sector

A search for rare decay of an Higgs boson into hidden sector has been produced by ATLAS [29], using $L=1.9 \text{ fb}^{-1}$. The decay chain considered is $H \rightarrow 2f_{d_2}$, where f_{d_2} is a fermion of the hidden sector, coupled to SM only via the Higgs sector. Then $f_{d_2} \rightarrow f_{d_1} \gamma_d$, where f_{d_1} is a second fermion of the hidden sector, lighter than f_{d_2} which escapes detection, and γ_d is a hidden photon, which eventually decays into $\gamma_d \rightarrow \mu\mu$. For particular values of mass of the γ_d , this particle is long-lived, so a displaced decay is expected. A scenario with $m_{\gamma_d} = 400 \text{ MeV}$ is considered, which provides a maximum of branching fraction $\mathcal{B}(\gamma_d \rightarrow \mu\mu) = 45\%$. The final state is a back-to-back pair of isolated, collinear, displaced μ^\pm . The presence of two escaping particles f_{d_1} does not gives much transverse

momentum imbalance since these two particles are back-to-back as well. No event has been found, and an upper limit on $\sigma\mathcal{B}(H \rightarrow 2\gamma_d + X) \lesssim 2 - 10$ pb as a function of the dark photon life-time $2 \lesssim (c\tau)_{\gamma_d} \lesssim 400$ mm has been set, as shown in Fig. 12. The same results can be interpreted as a lower limit on $\mathcal{B}(H \rightarrow 2\gamma_d + X) < 10\%$ for $7(5) < c\tau < 82(159)$ mm and for $m_H = 140(100)$ GeV.

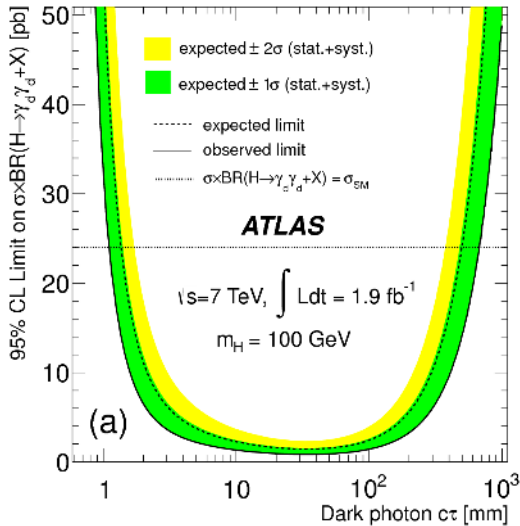


Figure 12. ATLAS exclusion plot at 95% for $\sigma\mathcal{B}(H \rightarrow 2\gamma_d + X)$ as a function of $(c\tau)_{\gamma_d}$ [29].

6 Summary

The experimental search for the Higgs sector at hadron colliders has been primarily focused on the search for SM Higgs boson. Other, extended scenarios beyond SM and MSSM have been also investigated, with a rich search program on many different final states. So far no significant excess has been observed, allowing to rule out most of the parameter space for SM4 and fermiophobic scenarios, and setting stringent limits on several NMSSM signatures as well as other more exotic models. The results of LHC experiments summarized in this paper include, in most of the cases, only the data collected at $\sqrt{s} = 7$ TeV, and only a fraction of that at $\sqrt{s} = 8$ TeV. So future updates of the analysis, as well as new searches, could yet reveal signs of physics beyond SM. Eventually, the LHC upgrade at $\sqrt{s} = 14$ TeV will largely extend the reach of all the searches to an higher energy.

References

- [1] CMS Collaboration, Phys. Lett. B **716**, 30 (2012), 1207.7235
- [2] ATLAS Collaboration, Phys. Lett. B **716**, 1 (2012), 1207.7214
- [3] CDF Collaboration, NIM A **271**, 387 (1988)
- [4] D0 Collaboration, NIM A **565**, 463 (2006)
- [5] ATLAS Collaboration, JINST **3**, S08003 (2008)
- [6] CMS Collaboration, JINST **3**, S08004 (2008)
- [7] G.D. Kribs, T. Plehn, M. Spannowsky, T.M.P. Tait, Phys. Rev. D **76**, 075016 (2007)
- [8] CDF and D0 and TEVNPH Working Group Collaborations (2011), 1108.3331
- [9] ATLAS Collaboration (2011), ATLAS-CONF-2011-135, <http://cds.cern.ch/record/1383838>
- [10] CMS Collaboration (2012), CMS-PAS-HIG-12-008, <http://cdsweb.cern.ch/record/1429928>
- [11] LEP Higgs Working Group, ALEPH, DELPHI, L3, and OPAL Collaborations (2001), hep-ex/0107035
- [12] CDF and D0 Collaborations and the Tevatron New Physics and Higgs Working Group, FERMILAB-CONF-11-413-E (2011), arXiv/1109.0576
- [13] ATLAS Collaboration, Eur. Phys. J. **C72**, 2157 (2012), 1205.0701
- [14] CMS Collaboration (2012), CMS-PAS-HIG-12-022, <http://cdsweb.cern.ch/record/1461937>
- [15] M. Maniatis, Internat. J. Modern Phys. **A25**, 3505 (2010)
- [16] B.A. Dobrescu, K.T. Matchev, JHEP **2000**, 31 (2000)
- [17] CDF Collaboration, Phys. Rev. Lett. **107**, 031801 (2011)
- [18] CMS collaboration (2012), CERN-PH-EP-2012-292, <http://cds.cern.ch/record/1490272>
- [19] D0 Collaboration, Phys. Rev. Lett. **103**, 061801 (2009)
- [20] A. Falkowski, J. Ruderman, T. Volansky, J. Zupan, JHEP **2010**, 1 (2010)
- [21] CDF Collaboration, Eur. Phys. J. **C62**, 319 (2009), 10.1140/epjc/s10052-009-1057-4
- [22] CMS Collaboration (2012), CMS-PAS-HIG-12-004, <http://cdsweb.cern.ch/record/1430019>
- [23] ATLAS collaboration (2012), ATLAS-CONF-2012-079, <http://cds.cern.ch/record/1460391>
- [24] M. Magg, C. Wetterich, Phys. Lett. B **94**, 61 (1980)
- [25] ATLAS Collaboration (2012), cERN-PH-EP-2012-265, <http://cds.cern.ch/record/1486012>
- [26] CMS Collaboration (2012), cMS-PAS-HIG-12-005, <http://cdsweb.cern.ch/record/1430020>
- [27] D0 Collaboration, Phys. Rev. Lett. **108**, 021801 (2012)
- [28] CDF Collaboration, Phys. Rev. Lett. **107**, 181801 (2011)
- [29] ATLAS Collaboration (2012), CERN-PH-EP-2012-241